

CHAPMAN PROFILE APPROACH FOR 3-D GLOBAL TEC REPRESENTATION

J. Feltens
EDS Industrien (Deutschland) GmbH, based at
Flight Dynamics Division,
ESA, European Space Operations Centre,
Robert-Bosch-Str. 5, D-64293 Darmstadt, Germany

ABSTRACT

Until now, ESOC employed single layer algorithms to describe ionospheric TEC 2-dimensionally. Since the real ionosphere is a 3-dimensional phenomenon but not a 2-dimensional one, the idea arose to establish a physically more realistic 3-dimensional model, based on a Chapman Profile approach. The presentation of this new 3-dimensional TEC model will be the task of this paper.

The new 3-dimensional TEC model represents the ionosphere's electron density by a simple Chapman Profile, whereby the layer of maximum electron density N_0 acts as scaling factor and its height h_0 as profile parameter. N_0 and h_0 in turn are modeled as global single layers. The 3-dimensional TEC model uses so called "leveled TEC observables", derived from dual-frequency GPS tracking data, for the determination of its model parameters in a least squares fit. Beyond the evaluation of ground-based tracking data, the processing of SST data is possible too.

INTRODUCTION

This paper will concentrate on the presentation of the basic mathematical algorithms that were worked out to realize a 3-dimensional Chapman Profile TEC model. Numerical results and analyses obtained during an application of the new model to TEC observation data over a longer period of time, are presented in the paper "*Routine Production of Ionosphere TEC Maps at ESOC - First Results*" (Feltens et al., 1998), which is also part of these IGS workshop proceedings.

The presentation of mathematical algorithms in this paper had to be limited to an overview only. A complete mathematical description of the 3-dimensional Chapman Profile TEC model with all its background is given in (Feltens, 1998), and everything what can only be shown roughly here, is described in (Feltens, 1998) in detail.

This paper will start with the attempt to express GPS-derived leveled TEC observables mathematically in terms of a 3-dimensional TEC model based on a Chapman Profile. Since TEC observables do not stand for discrete ionospheric electron density values at certain

points, but represent the integral over all electron densities along the satellite signal path, solutions of the analytical integral over several forms of the Chapman Profile function will be presented. The basic Chapman Profile model parameters are the maximum electron density N_0 and its height h_0 . They will be modeled as global single layers. Key points of numerical applicability for practical use are geometrical aspects, the setting up of linearized observation equations and the establishment of initial values needed for least squares fits. Finally this paper will give some remarks on the estimability of N_0 and h_0 from pure TEC observables and then close with a conclusion.

CONCEPTION OF A CHAPMAN PROFILE MODEL

A TEC observable can mathematically be described as follows:

$$S \cdot (\tilde{\Phi}_1 - \tilde{\Phi}_2)_j^i = TEC_j^i + S \cdot c \cdot (d_j + d^i) + \varepsilon \quad (1)$$

where

$S \cdot (\tilde{\Phi}_1 - \tilde{\Phi}_2)_j^i$	carrier phase leveled to code observable or “TEC observable” measured between satellite i and ground station (or second satellite) j ,
$S = 9.52$ [TECU/m]	multiplication factor for GPS signals, for details see Equation (4.5) of TN-08 (Feltens, 1995a),
TEC_j^i	slant range TEC along signal path from satellite i to station (satellite) j ,
$S \cdot c$	$S \cdot c = 2.85$ [TECU/s] multiplication factor to convert from [nanoseconds] into [TECU], for details see Equation (4.11) of TN-08,
d_j	differential hardware delay of station (or second satellite) j , normally given in [nanoseconds],
d^i	differential hardware delay of satellite i , normally given in [nanoseconds],
ε	TEC observation noise.

The Total Electron Content TEC is the integral of ionospheric electron density N_e along signal path:

$$TEC = \int_j^i N_e(s) ds \quad (2)$$

According to (Cappellari et al., 1976, page 7-46), the electron density N_e can at any point be represented as a function of height h_m and peak electron density N_m using a Chapman Profile:

$$N_e(z) = N_m \cdot e^{(1-z-e^{-z})} \quad \text{with} \quad z = \frac{h-h_m}{H} \quad (3)$$

where

N_e	electron density at any arbitrary point along the Chapman Profile,
h	height above Earth surface at which N_e is wanted,
N_m	maximum electron density of the Chapman Profile,
h_m	height of maximum electron density N_m above Earth surface,
H	scale height.

N_m and h_m vary with the zenith angle χ of the Sun, i.e. with day time (see e.g. Ratcliffe, 1972). At noon N_m reaches its maximum and h_m its minimum. And during the time from sunset to sunrise h_m has its maximum and N_m its minimum. To achieve more generality it's convenient to refer Equation (3) to the values that N_m and h_m would reach at noon time. With $N_m(\chi = 0^\circ) = N_0$ and $h_m(\chi = 0^\circ) = h_0$ Equation (3) can be expressed as follows in terms of N_0 and h_0 (Ratcliffe, 1972):

$$N_e(z) = N_0 \cdot e^{(1-z-\sec\chi \cdot e^{-z})} \quad \text{with} \quad z = \frac{h-h_0}{H} \quad (4)$$

where

χ	solar zenith distance,
N_0	maximum electron density of the Chapman Profile referred to $\chi = 0^\circ$,
h_0	height of maximum electron density N_0 above Earth surface at $\chi = 0^\circ$.

The Chapman Profile theory assumes the scale height to be constant along the whole profile (Ratcliffe, 1972). According to (Cappellari et al., 1976) the scale height can be expressed as a function of h_0 as follows:

$$H = \frac{5}{3} \cdot \{30 + 0.2 \cdot (h_0 - 200)\} = \frac{h_0 - 50}{3} \quad [km] \quad (5)$$

Once N_0 and h_0 are known, Equation (4) can be used to calculate the electron density at any point and height along the Chapman Profile. Putting Equation (4) into Equation (2) and this into Equation (1) gives finally Equation (6) relating the Chapman Profile to the TEC observable:

$$S \cdot (\tilde{\Phi}_1 - \tilde{\Phi}_2)_j^i = N_0 \int_j^i e^{(1-z-\sec\chi \cdot e^{-z})} ds + S \cdot c \cdot (d_j + d^i) + \varepsilon \quad (6)$$

Next a relation between the integrand ds and the profile variable z must be established: The differential triangle in Figure 1 indicates the following relation between differential increments dh in height and ds in slant range direction:

$$ds = \frac{dh}{\cos Z} \quad (7)$$

where

$\cos Z$

cosine of slant range zenith distance.

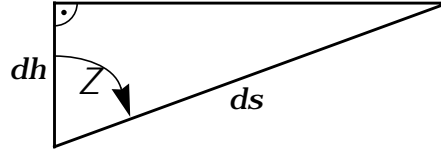


Figure 1: Differential triangle - relation between differential increment dh in height and differential increment ds in slant range direction.

And from Equation (4) the following relation between dz and dh can be derived:

$$dh = H \cdot dz \quad (8)$$

With the Relations (7) and (8) Equation (6) can thus be modified according to:

$$S \cdot (\tilde{\Phi}_1 - \tilde{\Phi}_2)_j^i = N_0 \cdot H \cdot \frac{1}{\cos Z} \cdot \int_{z_j}^{z_i} e^{(1-z-\sec\chi \cdot e^{-z})} dz + S \cdot c \cdot (d_j + d^i) + \varepsilon \quad (9)$$

The $1/\cos Z$ -term can be understood as counterpart to the mapping functions used for single layer models (see e.g. Feltens, 1995a).

For several versions of the Chapman Profile function analytical integrals were found. The establishment of these integrals is presented in detail in (Feltens, 1998). Since such formulae developments are out of the scope of this paper, only the final integral functions can be presented here.

Analytical integral over the simplest form of the Chapman Profile function:

$$\int e^{(1-z-e^{-z})} dz = e^{(1-e^{-z})} \quad (10)$$

The Integral (10) was also confirmed by (Cappellari et al., 1976), where it is inherent in the Equations (7-146).

Analytical integral over the $\sec\chi$ -form of the Chapman Profile function:

$$\int e^{(1-z-\sec\chi \cdot e^{-z})} dz = \cos\chi \cdot e^{(1-\sec\chi \cdot e^{-z})} \quad (11)$$

Analytical integral over the $\sec\chi$ -form of the Chapman Profile function in terms of height h above ground:

$$\int e^{(1-\left(\frac{h-h_0}{H}\right)-\sec\chi \cdot e^{-\left(\frac{h-h_0}{H}\right)})} dh = H \cdot \cos\chi \cdot e^{(1-\sec\chi \cdot e^{-\left(\frac{h-h_0}{H}\right)})} \quad (12)$$

Only the $\sec\chi$ -form of the Chapman Profile function is of relevance for further considerations. Regarding the Integrals (11) and (12), Equation (9) can finally expressed as follows:

$$S \cdot (\tilde{\Phi}_1 - \tilde{\Phi}_2)_j^i = N_0 \cdot H \cdot \frac{\cos \chi}{\cos Z} \cdot e^{(1 - \sec \chi \cdot e^{-\gamma}) \left(\frac{z_i}{z_j} \right)} + S \cdot c \cdot (d_j + d^i) + \varepsilon \quad (13)$$

Equation (13) is that final equation which relates TEC observables to the integral over the Chapman Profile. Equation (13) is thus the base upon which the observation equations will be set up.

REPRESENTATION OF N_0 AND h_0 AS SINGLE LAYERS

N_0 and h_0 are clearly coupled with $\chi = 0^\circ$, i.e. with noon time (see Equation (4) above). So the coordinate origin for N_0 / h_0 single layer development should be positioned at 12^h local time, i.e. at the Sun's maximum elevation above horizon. However, from ionosphere observations it is well known, that the diurnal maximum of electron density appears with a delay of about 2 hours. This effect has been accounted for in the software by calculating the Sun's position vector with a delay of 2 hours in such a way, that at 14^h the Sun's position of 12^h enters into the processing.

The software tests have shown that N_0 can be best modeled with a GE-function (Feltens, 1995b). And these software tests also confirmed the method of computing the solar ephemerides with a 2 hours delay, since the maxima of the fitted N_0 -GE-function and the Chapman Profile geometry ruled by χ did coincide under these conditions, thus causing the *rms* to minimize.

To model h_0 , special functions had to be worked out which force h_0 to get values in a predefined height range only. Two basic aspects had to be considered: 1) h_0 shall be modeled as smooth surface. 2) The surface functions should be designed so, that they can only reach values within predefined height limits. Since h_0 is referred $\chi = 0^\circ$, i.e. noontime, of the daily height variation, only the noontime values are of relevance for h_0 . Thus ignoring the daytime dependency, h_0 should only show variations depending mostly on solar activity. Expressed in numbers, these variations are in the range of $250 \leq h_0 \leq 400 \text{ km}$. However, the software tests have shown that the allowed height range should be set even narrower and slightly higher than 400 km :

$$h_{0_{min}} = 400 \text{ km} \quad , \quad h_{0_{max}} = 450 \text{ km} \quad , \quad \Delta h_0 = h_{0_{max}} - h_{0_{min}} = 50 \text{ km} \quad (14)$$

In operational use the allowed height range, as defined above in (14), should be adapted to the actual solar activity from time to time.

Of several candidates tried out, only the following approach, which appeared to be the most promising function to represent h_0 , is shown here. (Feltens, 1998) gives a complete overview over all candidates that were tried out for h_0 -modeling. The best candidate is a *sin*-function enclosing another function $f(x,y)$ as its argument. The *sin*-function restricts the output values always to the range $-1 \leq \text{value} \leq 1$, and the internal function $f(x,y)$ causes -

if not linear - the unknown parameters not to be affected by a 2π -bias, the period of the *sin*-function, which could make convergence unstable. h_0 is then established by a proper scaling of the extended *sin*-function:

$$h_0 = \xi(x, y) = h_{0_{min}} + \frac{\Delta h_0}{2} \cdot \{1 + \sin[f(x, y)]\} \quad (15)$$

Instead of a *sin*-function, a *cos*-function could have been used too. But, since both should be equivalent, only the *sin*-function approach was implemented into the software.

Of several candidates the one shown in Equation (16) was chosen for the inner function $f(\mathbf{x}, \mathbf{y})$. The first term $C \cdot \sin(x + y)$ has been included to enhance numerical stability:

$$f(x, y) = C \cdot \sin(x + y) + v_x \cdot \sin^2 x \cdot \cos x + \mu_x \cdot \sin x \cdot \cos^2 x + v_y \cdot \sin^2 y \cdot \cos y + \mu_y \cdot \sin y \cdot \cos^2 y \quad (16)$$

with

$$C = 0.001 \quad \text{numerically small constant}$$

And the arguments \mathbf{x} and \mathbf{y} are defined as follows:

$$\begin{aligned} +90^\circ \geq x \geq -90^\circ & \quad , \quad x = \Phi_m \\ 0^\circ \leq y \leq 180^\circ & \quad , \quad y = \tau/2 \end{aligned} \quad (17)$$

where

Φ_m geomagnetic latitude,
 τ local time.

The extended *sin*-function approach in the form presented above allows for the estimation of exactly 4 coefficients v_x, μ_x, v_y, μ_y . A generalization of Function (16) appears possible, but was not considered further. This might be a subject of future model extensions.

NUMERICAL REALIZATION

Integration of the Chapman Profile Formulae

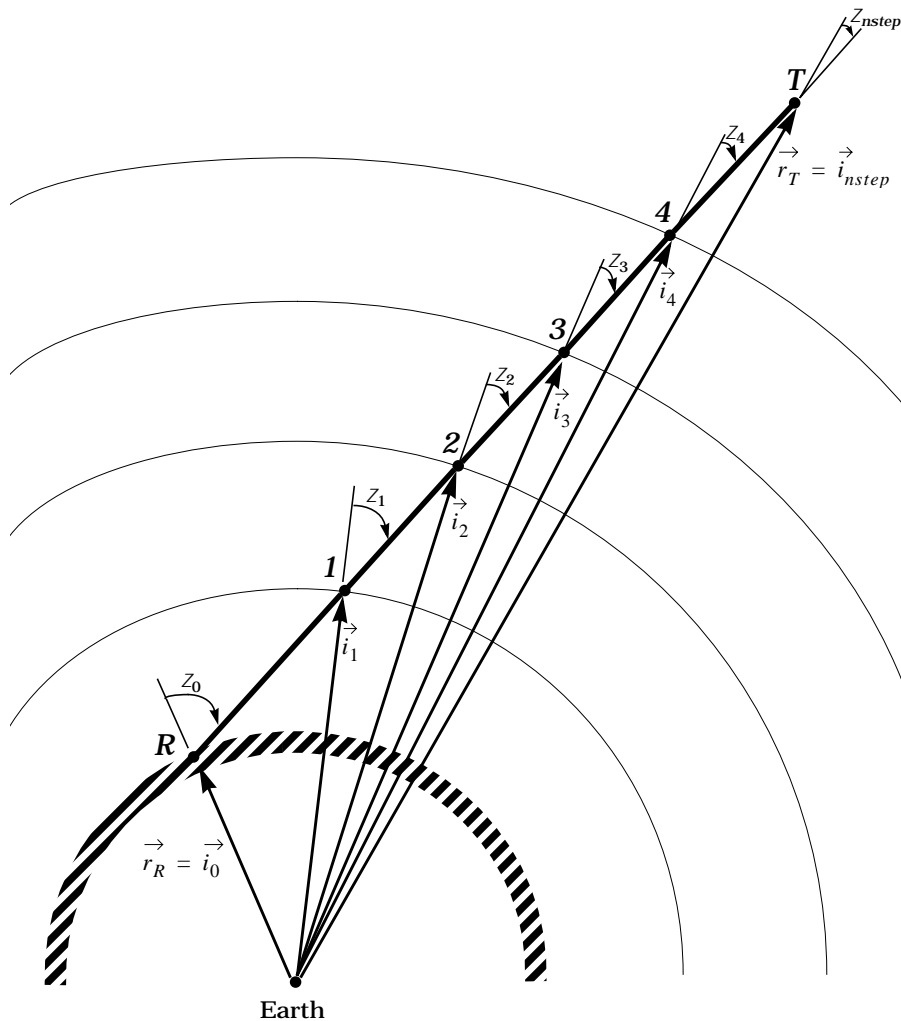


Figure 2: Change of zenith distance Z with height h .

In order to prepare the formulae of the preceding chapters for practical use, several aspects had to be considered:

- 1) The Integrals (11) and (12) were established under the assumption of plane stratified ionosphere layers, i.e. the satellite and solar zenith angles Z and χ were assumed to be constant and independent of height - but the real ionosphere is, like the Earth, in first approximation a sphere.
- 2) The 3-dimensional TEC model shall also be usable for satellite-to-satellite tracking (SST) data. In the case of ground-based GPS tracking it is obvious that ionospheric signal delays can be expressed by one Chapman Profile. - However, at SST applications

geometrical conditions can arise, at which an ionospheric delay must be expressed by the sum of two Chapman Profiles.

- 3) (Feltens, 1995a, Section 5.3) presents a method to determine position vectors of satellite signal intersection points through the layer of maximum electron density. This algorithm assumes the shell height to be globally constant. However, the new model treats h_0 as single layer, i.e. there are variations in height, depending on geographic position. So the formulae of (Feltens, 1995a) must here be used in an iteration loop to find an intersection point through the N_0 -layer.

Figure 2 shows how the satellite zenith distance Z changes with height h . The signal path is described by the range vector $\vec{\rho} = \vec{r}_T - \vec{r}_R$. In order to account for the changing satellite zenith distance Z , the following integration rule is exploited for Chapman Profile integration (see e.g. Bronstein and Semendjajew, 1979):

$$\int_a^d f(x)dx = \int_a^b f(x)dx + \int_b^c f(x)dx + \int_c^d f(x)dx \quad , \quad a < b < c < d \quad (18)$$

The signal path s along which to be integrated is thus subdivided into equidistant intervals ΔS . However, the signal path length is normally not an integer number of a predefined interval ΔS . So the “actual integration step width” Δs is defined as follows:

$$nstep = int\left(\frac{s}{\Delta S}\right) + 1 \quad \text{and} \quad \Delta s = \frac{s}{nstep} \quad [km] \quad (19)$$

where

s	slant range, identical with the amount $ \vec{\rho} $ of the range vector above,
ΔS	“nominal integration step width”,
$nstep$	number of integration steps,
int	function corresponding to Fortran INT, i.e. cutting off the decimal digits,
Δs	“actual integration step width”.

Integration is now done, starting at the lowest point of integration path and going upwards in steps of Δs to the highest point, in the way that at the beginning and ending of each interval Δs the position vectors \vec{i}_p on the slant range are determined:

$$\vec{i}_p = \vec{i}_0 + \frac{p \cdot \Delta s}{|\vec{\rho}|} \cdot \vec{\rho} \quad , \quad p = 1, 2, \dots, nstep \quad (20)$$

where (see Figure 2)

\vec{i}_p	position vector of an integration step beginning/ending point on slant range,
\vec{i}_0	position vector of the lowest point of the integration path,
\vec{i}_{nstep}	position vector of the highest point of the integration path,
$\vec{\rho}$	range vector defining slant range signal path $\vec{\rho} = \vec{r}_T - \vec{r}_R$,

Δs “actual integration step width”,

p running integration step number,

$nstep$ total number of integration steps.

Making the dot product of a position vector \vec{i}_p with the range vector $\vec{\rho}$ gives the cosine of the satellite’s zenith distance Z_p at that point p on the slant range:

$$\cos Z_p = \frac{\vec{i}_p \cdot \vec{\rho}}{|\vec{i}_p| \cdot |\vec{\rho}|} \quad (21)$$

And from the cosine values of two successive points p and $p-1$ the means are built:

$$\cos Z_{p-1,p} = \frac{1}{2} \cdot (\cos Z_{p-1} + \cos Z_p) \quad (22)$$

What was shown in Figure 2 for the satellite zenith distance is in a similar way also valid for the Sun’s zenith distance χ . So the solar zenith distance is handled in the same way as the satellite zenith distance was treated above: At each point \vec{i}_p where $\cos Z_p$ is computed, $\cos \chi_p$ is calculated too:

$$\cos \chi_p = \frac{\vec{i}_p \cdot (\vec{r}_* - \vec{i}_p)}{|\vec{i}_p| \cdot |\vec{r}_* - \vec{i}_p|} \quad (23)$$

where

\vec{r}_* the Sun’s position vector.

The mean value being valid for the integration step between two successive points p and $p-1$ is then:

$$\cos \chi_{p-1,p} = \frac{1}{2} \cdot (\cos \chi_{p-1} + \cos \chi_p) \quad \text{and} \quad \sec \chi_{p-1,p} = 1 / \cos \chi_{p-1,p} \quad (24)$$

On the other hand there is a significant difference between handling satellite zenith distances Z and solar zenith distances χ : Close to the terminator the Sun’s zenith angle becomes $\chi = 90^\circ$, and beyond on the nightside $\chi > 90^\circ$. This causes the $\sec \chi$ -term to become infinite at 90° and to change its sign beyond. The software tests have shown, that, when χ is approaching 90° , it should be frozen from a certain limit on for the whole nightside to a constant value. Of several values tried out $\chi = 70^\circ$ was found to be the best limit angle, i.e. for TEC modeling it is assumed that the electron content enclosed by the Chapman Profile does not go below that of $\chi = 70^\circ$ for the whole nighttime:

$$\text{If } \chi > 70^\circ \quad \rightarrow \quad \text{set } \chi = 70^\circ \quad (25)$$

The software tests have shown that the Chapman Profile integration should be restricted to a height range of **60 - 2000 km**. As appropriate step width $\Delta S = 50 \text{ km}$ was identified. Before starting the integration, the software reduces integration path to that part of the whole slant range from ground station to satellite, which lies in that height range.

Establishment of Linearized Observation Equations

In order to obtain the partials with respect to the unknowns Equation (13) is written here again, now with the functional dependencies explicitly expressed:

$$S \cdot (\tilde{\Phi}_1 - \tilde{\Phi}_2)_j^i = N_0 \cdot H(h_0) \cdot \frac{\cos \chi}{\cos Z} \cdot e^{(1 - \sec \chi \cdot e^{-z(h_0, H(h_0))}) \frac{z_j}{z_j}} \Big|_{z_j}^{\tilde{z}_j} + S \cdot c \cdot (d_j + d^i) + \varepsilon \quad (26)$$

and

$$z(h_0, H(h_0)) = \frac{h - h_0}{H(h_0)}, \quad H(h_0) = \frac{h_0 - 50}{3} \text{ [km]}$$

The unknowns to be estimated in Equation (26) are the single layer coefficients N_{kl} and h_{nm} to represent $N_0(N_{kl})$ and $h_0(h_{nm})$, and the differential code bias values d_j and d^i . For the single layer coefficients N_{kl} and h_{nm} the partials $\partial\{S \cdot (\tilde{\Phi}_1 - \tilde{\Phi}_2)\}/\partial N_0$ and $\partial\{S \cdot (\tilde{\Phi}_1 - \tilde{\Phi}_2)\}/\partial h_0$ are needed anyway, and then the partials $\partial N_0/\partial N_{kl}$ and $\partial h_0/\partial h_{nm}$ are attached via chain rule to obtain the required partials $\partial\{S \cdot (\tilde{\Phi}_1 - \tilde{\Phi}_2)\}/\partial N_{kl}$ and $\partial\{S \cdot (\tilde{\Phi}_1 - \tilde{\Phi}_2)\}/\partial h_{nm}$ with respect to the unknowns needed for the observation equations. Knowledge of the partials $\partial\{S \cdot (\tilde{\Phi}_1 - \tilde{\Phi}_2)\}/\partial N_0$ and $\partial\{S \cdot (\tilde{\Phi}_1 - \tilde{\Phi}_2)\}/\partial h_0$ thus allows for the establishment of the partials for coefficients of any single layer model by applying the chain rule. Exploiting this fact, any single layer model can be extended for 3-dimensional Chapman Profile applications.

Regarding the geometrical aspects treated in the previous section and Equation (26), the TEC and its partial with respect to h_0 , which are both obtained via integration along the profile, can be expressed by the following summation formulae for practical use:

$$TEC(h) = N_0 \cdot H \cdot \sum_{p=1}^{nstep} \frac{1}{\cos Z_{p-1,p}} \cdot \left\{ \cos \chi_{p-1,p} \cdot e^{(1 - \sec \chi_{p-1,p} \cdot e^{-z_p})} - \cos \chi_{p-1,p} \cdot e^{(1 - \sec \chi_{p-1,p} \cdot e^{-z_{p-1}})} \right\} \quad (27)$$

and

$$\begin{aligned} \frac{\partial TEC(h)}{\partial h_0} &= \frac{N_0}{3} \cdot \sum_{p=1}^{nstep} \frac{1}{\cos Z_{p-1,p}} \cdot \left\{ \cos \chi_{p-1,p} \cdot e^{(1 - \sec \chi_{p-1,p} \cdot e^{-z_p})} - \cos \chi_{p-1,p} \cdot e^{(1 - \sec \chi_{p-1,p} \cdot e^{-z_{p-1}})} \right\} \\ &+ N_0 \cdot H \cdot \sum_{p=1}^{nstep} \frac{1}{\cos Z_{p-1,p}} \cdot \left\{ e^{(1 - z_p - \sec \chi_{p-1,p} \cdot e^{-z_p})} \cdot \frac{\partial z_p}{\partial h_0} - e^{(1 - z_{p-1} - \sec \chi_{p-1,p} \cdot e^{-z_{p-1}})} \cdot \frac{\partial z_{p-1}}{\partial h_0} \right\} \end{aligned} \quad (28)$$

and the partials $\partial z_{p-1}/\partial h_0$ and $\partial z_p/\partial h_0$, being needed for Summation Formula (28):

$$\frac{\partial z_{p-1}}{\partial h_0} = \frac{-1}{H} \cdot \left\{ 1 + \frac{z_{p-1}}{3} \right\} \quad \text{and} \quad \frac{\partial z_p}{\partial h_0} = \frac{-1}{H} \cdot \left\{ 1 + \frac{z_p}{3} \right\}$$

The partial $\partial TEC(h)/\partial N_0$ is trivial:

$$\frac{\partial TEC(h)}{\partial N_0} = \frac{TEC(h)}{N_0} \quad (29)$$

If, for a SST measurement, the total integration path must be sub-divided into two sub-paths, two Chapman Profiles have to be integrated, and the final partials with respect to N_0 and h_0 are then obtained by summing up the partials of each Chapman Profile.

The partials for the receiver and satellite differential code bias d_j and d^i are simply:

$$\frac{\partial\{S \cdot (\tilde{\Phi}_1 - \tilde{\Phi}_2)\}}{\partial d_j} = S \cdot c = 2.85 \text{ (for GPS)} \quad , \quad \frac{\partial\{S \cdot (\tilde{\Phi}_1 - \tilde{\Phi}_2)\}}{\partial d^i} = S \cdot c = 2.85 \text{ (for GPS)} \quad (30)$$

Getting Initial Values for the Unknowns

Since N_0 appears linear in the Chapman Profile function (see Equation (26)), its value needs not to be known a priori to establish the partial for it. Equation (29) shows that its partial is the TEC value normalized to N_0 . So using Equation (27) and summing up the TEC with $N_0 = 1$ gives the partial for N_0 without necessity of explicit knowledge of N_0 itself. However, a h_0 -value is needed to do this summation. During the first iteration h_0 is thus kept fixed to some initial values, and only values for the N_0 -single layer coefficients are estimated. If N_0 is represented by a GE-function, this first iteration must be done in logarithmic mode (Feltens, 1995b and Feltens, 1998). From the second iteration on the h_0 -parameters are then estimated together with the N_0 -parameters, using the N_0 -coefficient values obtained from the first (or the previous) iteration as initial values. In the case h_0 is represented by an extended *sin*-function, the h_0 -coefficients are kept fixed with one $(v_x)_0, (\mu_x)_0, (v_y)_0, (\mu_y)_0 = 1$ (with respect to the predefined height range given in Equation (14)) during the first iteration.

h_0 's role is twofold: On one hand it is estimated as an unknown, on the other hand it is used to fix the intersection points through the N_0 -layer in order to evaluate N_0 - and scale height H -values there, and to compute the argument z of the Chapman Profile function. To evaluate the intersection points, N_0 , H and z , the h_0 -single layer parameters of the previous iteration must thus be used. To make N_0 finally conform with h_0 , a last iteration is made with keeping h_0 again fixed, now to its recently estimated values, only estimating the N_0 -parameters and the differential code bias values.

ESTIMABILITY OF N_0 AND h_0 FROM TEC OBSERVABLES

The software tests have shown, that the Chapman Profile fits are rather insensitive against h_0 -variations, and estimated h_0 -parameters show only weak significance. This is obvious when keeping in mind that TEC observables are measurements of the integral over the electron density, and this integral is the area under the electron density profile. A TEC observable thus corresponds to such an area value. And an area value alone gives only the area's amount, saying nothing about the area's shape, i.e. the profile peak at h_0 can be extracted from the information provided by pure TEC observables only from effects caused by the varying elevations under which these observables were made. Because for lack of corre-

sponding tracking data, the SST option could not be included into the software tests so far. It is hoped that the inclusion of SST data will improve the situation, since SST measurements are affected, depending on the geometrical conditions, by more varying parts of the ionosphere than ground-based tracking data. Inclusion of SST data might thus improve the resolution of profile parameters, such as h_0 .

The determination of N_0 -parameters is stable, and N_0 -single layer coefficients are estimated significantly. TEC models obtained when modeling N_0 with GE-functions appear to have the same order of accuracy as pure single layer GE-function fits - with the *rms* tending to be slightly better, i.e. Chapman Profile fits are of comparable accuracy as pure GE-function fits, but provide information on the ionosphere's third dimension - the height.

CONCLUSIONS

A mathematical model has been worked out allowing for the 3-dimensional representation of ionospheric TEC from TEC observation fits. These TEC measurements can be derived from GPS dual-frequency tracking data. The ionospheric TEC is modeled as the integral over simple Chapman Profiles with the layer of maximum electron density N_0 acting as scaling factor and its height h_0 as profile parameter. Both, N_0 and h_0 , are in turn represented as global single layers. For the modeling of h_0 special single layer functions were developed.

Since GPS-derived TEC observables represent the ionosphere's total electron content along signal path, no discrete electron density values are observed, but the integral over all electron densities along the signal path. Analytical solutions for the integral over several versions of the Chapman Profile function were found and implemented into the model. In order to account for certain geometrical aspects, the integral over the Chapman Profile function is finally evaluated by a mixture of analytical and numerical approach.

From its conception this Chapman Profile-founded model allows the evaluation of ground-based data as well as of SST data. However, for lack of SST data, software tests had so far to be restricted to the evaluation of ground-based data.

All in all the whole 3-dimensional TEC model is built up by simple mathematical formulae. From the model's and the software's conception and structure it is possible to combine it with every single layer and to include more complex ionosphere profiles in future steps of software extension.

The task of this paper was the presentation of the basic mathematical algorithms realizing the 3-dimensional TEC model. Analyses of numerical results, that came out when applying this model to TEC data fits, are presented in (Feltens et al., 1998), which is also published in these IGS workshop proceedings.

REFERENCES

- Bronstein, I.N. and K.A. Semendjajew, 1979, Taschenbuch der Mathematik, *Verlag Harri Deutsch, Thun und Frankfurt/Main*, Vol 1+2.
- Cappellari, J.O, C.E. Velez and A.J. Fuchs, 1976, Mathematical Theory of the Goddard Trajectory Determination System, Goddard Space Flight Center, X-582-76-77, Greenbelt, MD, U.S.A., April 1976, Section 7.6.2 'Ionosphere Models', pp 7-44 - 7-52.
- Feltens, J., 1995a, GPS TDAF Ionosphere Monitoring Facility, Mathematical Model Developments, in *GTDAF-TN-08 Iss 1/- 11 Sep-95* (ESOC-internal document).
- Feltens, J., 1995b, GPS TDAF Ionosphere Monitoring Facility, Examination of the Applicability of Gauß-Type Exponential Functions to Ionospheric Modeling, in *GTDAF-TN-09 Iss 1/- 11 Sep-95* (ESOC-internal document).
- Feltens, J., 1998, GPS TDAF Ionosphere Monitoring Facility, Chapman Profile Model for the IONMON, in *GTDAF-TN-14 Iss 1/- 04 Mar-98* (ESOC-internal document).
- Feltens, J., J.M. Dow, T.J. Martín-Mur, C. García Martínez and P. Bernedo, 1998, Routine Production of Ionosphere TEC Maps at ESOC - First Results, IGS Presentation, in *Proceedings of the 1998 IGS Analysis Centers Workshop*, ESOC, Darmstadt, Germany, February 9-11, 1998.
- Ratcliffe, J.A., 1972, An introduction to the ionosphere and magnetosphere, *Cambridge University Press, Great Britain*, 1972.